

JERZY CIEŚLIK*, KATARZYNA GODYŃ**

MICROSCOPIC ANALYSIS OF SHEAR BANDS FORMATION IN LUNA LIMESTONE UNDER QUASISTATIC TRIAXIAL LOADING CONDITIONS

ANALIZA MIKROSKOPOWA PASM ŚCINANIA PRÓBEK WAPIENIA LUNA PODDANYCH QUASISTATYCZNYM TRÓJOSIOWYM OBCIĄŻENIOM

The article presents the results of microscopic analyses of shear bands of carbonate rocks subjected to triaxial compression. Strength tests were performed in axisymmetric loading conditions, at various confining pressures and strain rates. The layout and nature of phenomena occurring in shear bands at various strain rate loading conditions were analysed under the microscope on thin rock sections of damaged samples. The principal part of the study involves identification of damage types in shear bands, which mainly depend on the rock deformation rate and petrography. Also, quantitative analysis of particular types of damage in shear bands was performed and their dependence on the mechanical tests conditions. The last item discussed in this article is the quantitative analysis of the width of shear bands at various loading conditions.

Keywords: laboratory investigations, shear bands, microscopic analysis, quasistatic triaxial loading conditions

W artykule zaprezentowano wyniki analiz mikroskopowych pasm ścinania próbek skał węglanowych poddanych trójosiowemu ściskaniu. Testy wytrzymałościowe przeprowadzono w osiowo symetrycznym stanie obciążenia, przy różnych ciśnieniach okólnych oraz prędkościach obciążenia. Zniszczone próbki były przedmiotem analiz mikroskopowych na szlifach skalnych. Badano układ i charakter zjawisk występujących w pasmach ścinania przy różnych warunkach obciążenia. Zasadniczą część pracy stanowi identyfikacja typów zniszczenia w pasmach ścinania, zależnych w głównej mierze od prędkości odkształcenia i petrografii skały. Przeprowadzono również ilościową analizę udziału poszczególnych typów zniszczenia w pasmach ścinania oraz ich zależność od charakteru obciążeń mechanicznych. Ostatnim wątkiem poruszonym w artykule jest ilościowa analiza szerokości pasm ścinania przy różnych warunkach obciążenia.

Słowa kluczowe: badania laboratoryjne, pasma ścinania, analiza mikroskopowa, quasistatyczne trójosiowe obciążenia

* AGH UNIVERSITY OF SCIENCE AND TECHNOLOGY, FACULTY OF MINING & GEOENGINEERING, DEPARTMENT OF GEOMECHANICS, CIVIL ENGINEERING AND GEOTECHNICS, AL. A. MICKIEWICZA 30, 30-059 KRAKOW, POLAND, E-mail: jerz@agh.edu.pl

** STRATA MECHANICS RESEARCH INSTITUTE OF THE POLISH ACADEMY OF SCIENCES; UL. REYMONTA 27, 30-059 KRAKÓW, POLAND; E-mail: godyn@img-pan.krakow.pl

1. Introduction

Shear bands understood as narrow areas where permanent deformations are focused, which accompany rock damage by shearing, are often observed both in natural and laboratory conditions (Tondi et al., 2006; Desrues & Viggiani, 2004; Bésuelle et al., 2000; Ord et al., 1991; El Bied et al., 2002; Paterson & Wong, 2005; Gustkiewicz et al., 2007). Strongly deformed bands, often referred to as localization zones, occur in rocks mainly in the case of triaxial loading conditions. A characteristic feature of shear bands present in rocks is the change or destruction of initial structure of the rock, binding material, and structurally differing area. The nature of such changes, however, are different in rocks with high porosity, e.g. in some sandstones or limestone's (El Bied et al., 2002; Vajdova et al., 2010; Renner & Rummel, 1996), and different in hard, crystalline rocks with small porosity, such as granites (Amirano & Schmittbuhl, 2002; Wong, 1982), quartzite's or marbles (Hallbauer et al., 1973; Olsson & Peng, 1976).

In the first case, the mechanism and form of damage significantly depends on the hydrostatic component of the stress conditions according to which the load is exerted. At high confining pressure values, the entire sample undergoes uniform compaction without macroscopically observed shear band formation (Vajdova et al., 2010; Baud et al., 2000). It is also possible that some limited zone of compaction is formed, called the "compaction band" (Louis et al., 2006; Klein et al., 2001). Generally, such changes are caused by reduced porosity and the accompanying plastic, volumetric deformation due to collapse of the pore structure (Vajdova et al., 2010, Bésuelle et al., 2003).

At lower confining pressures, damage occurs by shear band, or many shear bands, while the band itself can undergo dilatancy or compaction (El Bied et al., 2002; Bésuelle, 2000, 2003; Wub, 2000; Vajdova et al., 2010). In such conditions, cataclasis is also a frequent phenomenon in the shear band.

In the case of hard, crystalline rocks, due to development of microcracks, shear bands are a result of crack coalescence, formed as a inclined zones, while at higher confining pressures are accompanied with cataclasis and dilatancy (Amirano & Schmittbuhl, 2002; Wong, 1982; Paterson & Wong, 2005; Hallbauer et al., 1973; Olsson & Peng, 1976). The process of crack nucleation and propagation occurs inside or between the grains and varies for various rock types. At small confining pressure values, damage can also occur in the form of a macro-crack, which comprises connected microcracks and fractures (Paterson & Wong, 2005). The dominating role in the process belongs to initial microcracks and microfractures oriented in the loading direction, which propagate in the form of "wing cracks".

Mathematical description of behaviour of materials undergoing damage in the form of shear bands or compaction is the theory of plasticity and bifurcation, which allows for determining loading conditions and properties of materials where particular forms of damage will occur (Rudnicki, 2004; Issen & Rudnicki, 2000). Experimental analysis of shear bands with various techniques and in various rock masses is, therefore, the object of interests for many researchers. Depending on the research techniques applied, one can analyse both their spatial orientation, e.g. with computer tomography techniques (Desrues & Viggiani, 2004; Desrues, 2004), as well as their nature and range – for this purpose optical or electron microscopes are usually used (El Bied et al., 2002; Paterson & Wong, 2005).

Spanish Luna limestone is a weak rock with high porosity (approx. 14%) which, when subjected to triaxial strain, depending on the confining pressure, can undergo damage both in

the form of uniform compaction for the entire sample, and in the form of shear bands (Table 1). In the aspect of physical and mechanical properties, it corresponds to Tavel limestone (Vajdova et al., 2010). In the case of damage in the form of shear bands, depending on strain rate, damage in one shear band can occur in the form of cataclasis, cracking between grains, compaction, or loosening of the rock material. The nature of such phenomena and their quantitative share depending on strain rate is the topic of this article.

2. Strength tests of Luna limestone samples

Strength tests were performed on cylindrical limestone samples with dimensions $\phi = 34$, $h = 70$ mm, cut from rock plate.

Axi-symmetrical load was applied at samples using the MTS triaxial cell type 656.11, and the strength test machine with stiff frame type MTS 315. The measurement of axial force was performed using force transducer installed inside the pressure chamber, while displacements were measured with extensometer. Radial displacements were determined by measurement of changes to sample circumference, with a chain surrounding it, while axial – outside the chamber, by measuring the displacements of the triaxial cell piston.

Depending on the applied confining pressure value, in place of fracture of limestone samples (Fig. 1), already at the pressure of $p = 5$ MPa damage occurred in the form of one, while in the case of circular pressure of $p = 10, 20$ MPa – in the form of many shear bands. Confining pressure $p = 40$ MPa corresponds to plastic deformation and ductile behaviour of samples without clearly developed shear bands (Fig. 1).



Fig. 1. Damage of the limestone samples in the form of (from the left): fracture for $p = 0$ MPa, single shear band $p = 5$ MPa, two shear bands $p = 20$ MPa, plastic yield $p = 40$ MPa (for better visualisation, negative of the photo has been presented)

In the confining pressure range of $p = 0, 5, 10, 20$ MPa, Luna limestone behaves in a brittle manner, becoming softening in the post-critical range (Fig. 2). At confined pressure of $p = 40$ MPa, the characteristics of differential strain in axial deformation, after breaching the strength limit, corresponds to ideally plastic behaviour.

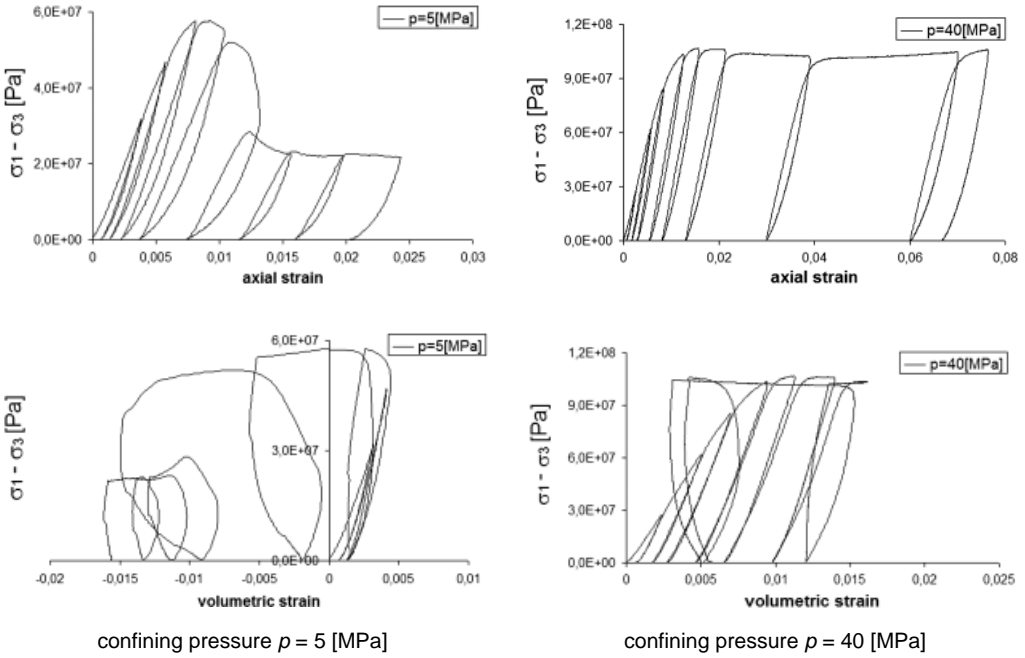


Fig. 2. Example characteristics $(\sigma_1 - \sigma_3) - \varepsilon$ obtained for confined pressure of 5 MPa and 40 MPa at deformation rate of $1 \times 10^{-4} [s^{-1}]$

The range of all tests covered tests performed for six confined pressures (0, 5, 10, 15, 20, 40 MPa) and four strain rates $\varepsilon = 1 \times 10^{-5} [s^{-1}]$, $1 \times 10^{-4} [s^{-1}]$, $5 \times 10^{-4} [s^{-1}]$, $1 \times 10^{-3} [s^{-1}]$, whereas the greatest deformation rates of $1 \times 10^{-3} [s^{-1}]$ were only applied for uniaxial tests (Fig. 3).

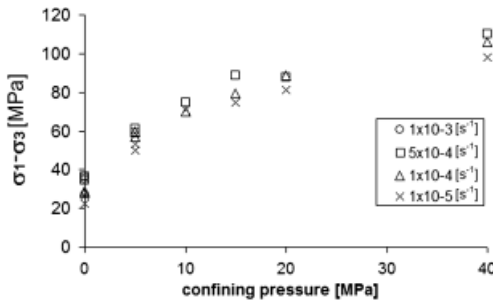






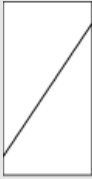







Fig. 3. The strength limit dependency (for differential stress) on confined pressure and deformation rate

The influence of strain rate on limestone limit strength is observed for all confined pressures, yet it is the most visible in uniaxial tests and confined pressure of $p = 5$ MPa.

Because sample damage in the form of shear bands was achieved for confined pressures not exceeding $p = 20$ MPa (the bands marked in drawings in Table 1 with slanting lines), microscopic analyses were performed for tests with confining pressure of $p = 5, 10$ and 20 MPa. Rock sections and then their analysis were performed for seven samples, three confined pressures and three deformation rates, which were schematically marked in Table 1 with dark background.

TABLE 1

Scope of microscopic analyses for Luna limestone (marked in grey)

Strain rate/ confining pressure	5 MPa	10 MPa	20 MPa	40 MPa
$1 \times 10^{-5} \text{ [s}^{-1}\text{]}$				
$1 \times 10^{-4} \text{ [s}^{-1}\text{]}$				
$5 \times 10^{-4} \text{ [s}^{-1}\text{]}$				

Thin sections were always made perpendicularly to the shear surface, with their longer edge oriented according to the load direction. Sections dimensions amounted to 40×20 mm

3. A petrographic description of limestone samples

The petrographic analyses were carried out by means of the AXIOPLAN polarization microscope produced by ZEISS. The samples, which had a form of thin sections, were examined in the transmitted light. The magnification was 50-200X.

The analyzed limestone deposits are characterized by a slightly porous, incoherent, grain-stone-type structure (Dunham, 1962). The rock matrix is composed of authigenic carbonate cements, built mostly of calcite and dolomite, and – sometimes – sulfates. The size of these components is ~ 0.1 - 0.3 mm. They have a form of irregular (xeromorphic) specimens or, less frequently, hipautomorphic specimens or rhombohedral crystals of the automorphic dolomite.

The rock skeleton is composed of various types of carbonate grains (mostly calcite ones), whose volume fraction is far more than 50 percent. They are oval (less frequently round), elon-

gated, and sometimes crumbled fragments of the deposit. These include micritized intraclasts, pellets, and ooids – and, sporadically, organic remains (the so-called bioclasts). Thus, according to the classification provided by Folk (1959), these rocks are included in the category of allochemical deposits. The average size of the allochemical components is ca. 0.2 mm, and their maximum size does not exceed 0.4 mm. This means that these grains should be classified as calcarenites (Folk, 1968). A small amount of rounded grains of the detritic quartz, of the size of 0.1-0.25 mm, is also present in the discussed rocks.

Among the grain components of the rocks and the carbonate cement, there is an unoccupied space that is decisive for the rock porosity. The size of pores usually does not exceed 0.1 mm.

4. Types of structural changes resulting from the mechanical load applied to the samples

The macroscopic effects of the mechanical load applied to samples and of the sample destruction can be observed as shear bands. Under a microscope, these bands reveal an area that is structurally different from the remaining part of the sample: it is highly deformed and, very often, composed of a rock material which has been transformed with respect to its original condition. Due to microscopic analyses, it was possible to examine these areas in detail and describe the nature of the phenomena occurring there. As a result, three types of phenomena were singled out. However, it is often difficult to determine the conditions in which they occur; also, sometimes their effects overlap.

4.1. Single, isolated cracks

This phenomenon occurs in the areas where the continuity of the rock has been disrupted, which most commonly results in the formation of single cracks of various width. In some cases, these cracks form an almost straight line (Fig. 4); in others, they are irregular (Fig. 5) and they

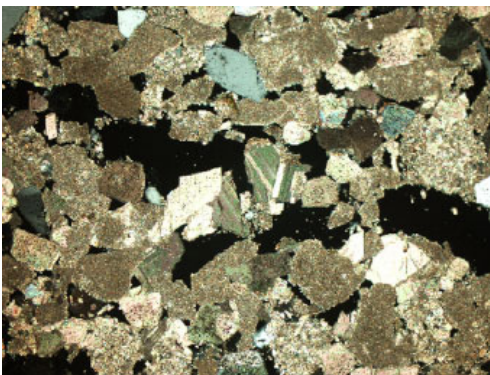


Fig. 4. A crack cutting through rock, forming an almost straight line. Magnification 100×, NX

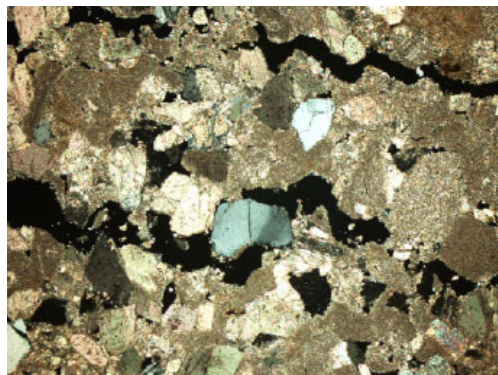


Fig. 5. A network of irregular cracks. In the central part of the crack, there can be seen a detritic, broken grain of quartz. Magnification 100×, NX

can be observed in between the mineral components which the rock is built of. In the spots where these cracks occur, the habits of crystals (such as rhombohedrons of dolomite) present in a given rock can be seen particularly clearly (Fig. 4). The width of the cracks and fissures is different in each sample – at the most, it can be 0.5 mm.

4.2. Compaction/loosening of the rock material

The scope of such areas is quite large (even several millimeters). In such areas, the carbonate authigenic cement and the granular components are pressed, or compacted (Fig. 6), and the original porosity of the rock material is significantly reduced. In other spots, the intergranular and intercrystalline space becomes loosened, which results in an increase in porosity (Fig. 7).

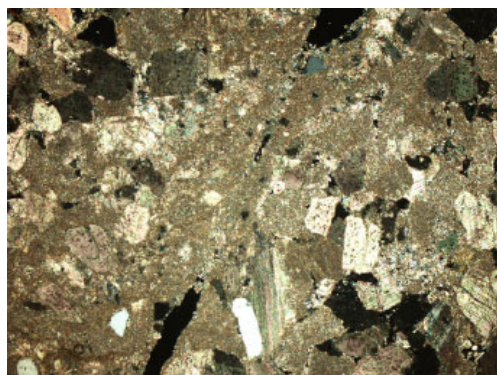


Fig. 6. A rock with a blurred original structure. A vestigial crack, surrounded by some highly pressed rock material (mostly micrites), can be observed. Magnification 100 \times , NX

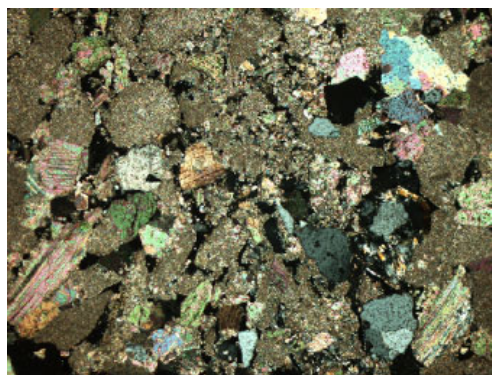


Fig. 7. An area structurally altered, built of micritic and sparitic carbonates and quartz. Grain-to-grain links have been significantly loosened, which resulted in an increase in porosity. Magnification 100 \times , NX

4.3. Shear in the form of cataclasis

This term, imprecise from the point of view of geology, is used to describe such phenomena as grinding, dislocation, and cementing of the deposit elements. In these areas, the authigenic crystals and the allogenic deposit elements are cemented and mixed to such an extent that sometimes it is difficult to describe such a piece of rock in an accurate way (Fig. 8). The impact of these phenomena brings about the most advanced structural changes observed in the analyzed samples.

A special case of such structural changes occurring on the brink of such phenomena is the situation in which a partly “cicatrizized” area appears where the crack should run through the rock. In such places, a markedly visible crack suddenly disappears – as if it got lost in the micritic rock – to reappear later, in some further section of the rock. Such a phenomenon is often accompanied by the occurrence of a highly pressed rock material or cataclasis (Fig. 9).

Apart from the phenomena described above, one can also observe changes in the original porosity of the rock, mostly in the area where the discussed phenomenon occurs, or close to it.

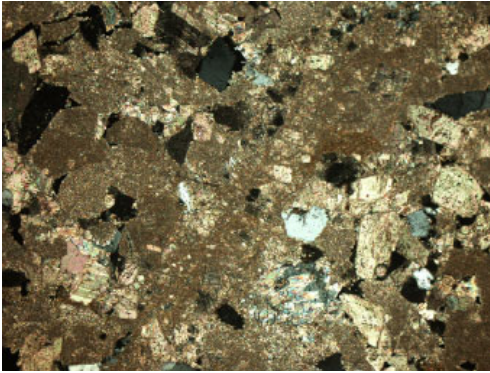


Fig. 8. An area highly altered structurally in which the broken continuity of the deposit, i.e. the cataclasis, is not visible. Magnification 100×, NX

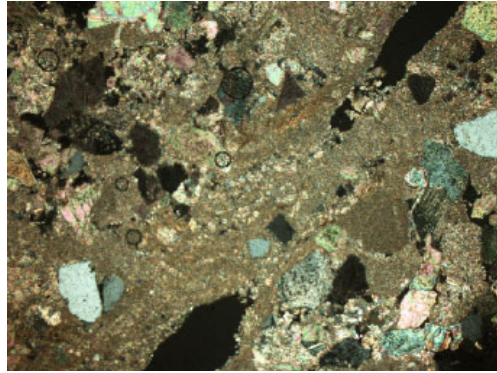


Fig. 9. An area highly altered structurally in which the “cicatrization” of the crack can be observed. The rock is composed of the micritic and sparitic substances, ground and mixed together. Magnification 100×, NX

Porosity increases when cracks are formed, or when the intergranular and intercrystalline space becomes loosened. When the micritic-sparitic material is grounded, dislocated and pressed, porosity decreases significantly.

4.4. The relation between the petrographic characteristics of the analyzed rocks and the structural changes

During the petrographic analysis of the samples, it was observed that there exists a certain relationship between the petrographic characteristics of the analyzed rocks and the nature of the structural changes occurring in them. The analyzed rock samples are built of a petrographically heterogeneous material – and the characteristics which influence the nature and scope of the structural changes result from this heterogeneity of the mineral composition, structure/texture, or from the origins of the deposit. The qualitative description of this phenomenon, difficult to describe in a quantitative manner, is provided below.

One factor that is conducive to the occurrence of structural changes in the form of **the compaction/loosening** of the intercrystalline and intergranular space is the presence of **the carbonate cement**. In the areas where the carbonate cements occurred, there were **cracks** that ran through rocks not damaging their structure (or causing just a partial damage). In such areas, cataclasis was observed less frequently.

The main component of the analyzed limestone samples is a material which consists mostly of **micritic carbonate grains** bonded with the authigenic cement. In such areas, the main crack is surrounded by some **pressed and compacted carbonate material**, which results in the diminishing of the intergranular or intercrystalline space. In some spots, the original structures are almost totally blurred, which results in the formation of “**cataclasis**” (Fig. 8).

In the course of the microscopic observations, the presence of **the detritic quartz** in the deposit was also revealed. Due to its high durability, it suffers just minor damages. Sporadically, one can observe in it single cracks (Fig. 10), or a more elaborate network of cracks (Fig. 11).

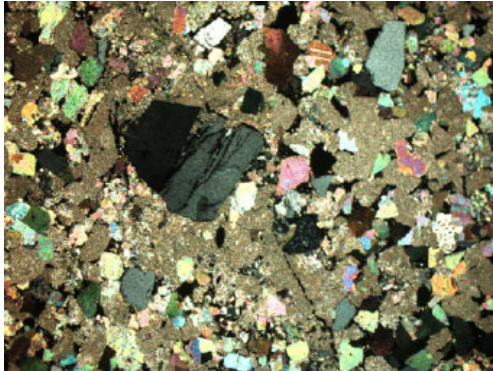


Fig. 10. A grain of fractured quartz in a “structurally altered” area. Magnification 50×, NX

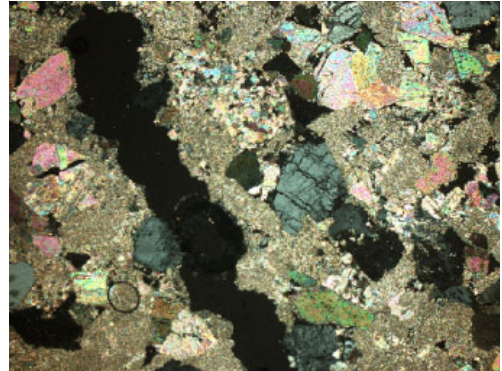


Fig. 11. A crack surrounded by visible micritic crumbs and carbonate cements, and highly fractured quartz grains. Magnification 100×, NX

5. Quantitative assessment of phenomena occurring in shear bands

In the macroscopic assessment, shear bands form surfaces appropriately slanted against the greatest loading direction. When analysing this phenomenon in the microscopic scale, it must be stated that within a single shear band (for one sample), in its various segments, one can observe different types of structural changes that decide on the form of damage.

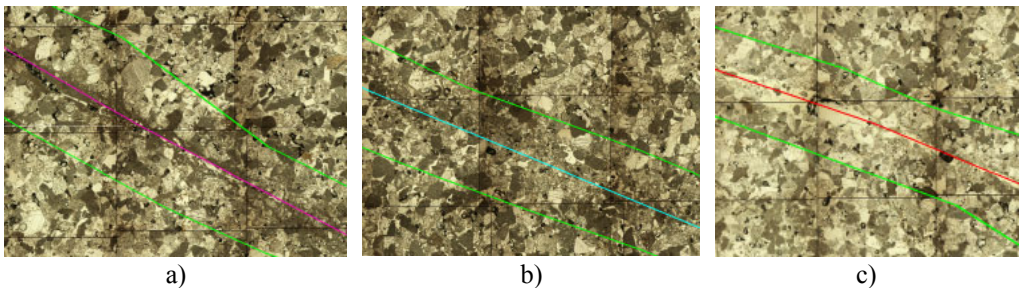


Fig. 12. Examples of different forms of structural changes observed in sample shear bands. Each drawing includes several microscopic images


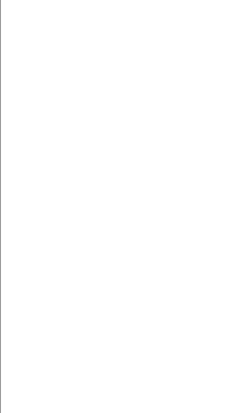
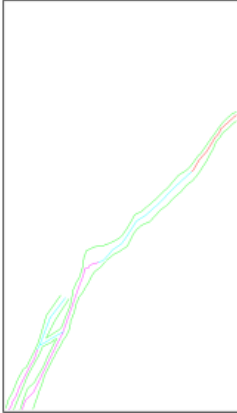
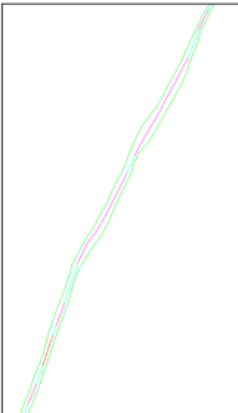
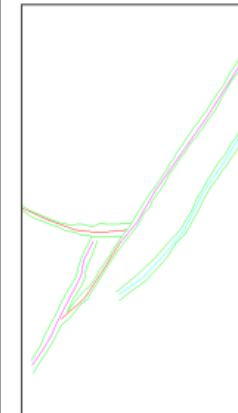
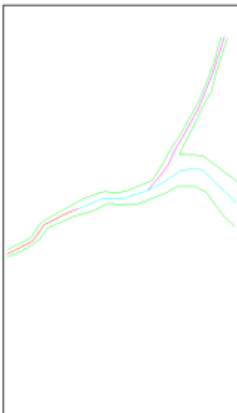
In Figure 12, examples of different structural changes have been marked with different colours: a) in the form of cataclasis, b) in the form of compaction/loosening of grains, c) in the form of single fracture. Apart from the aforementioned forms of damage, not far from the phenomena discussed, one can also observe the change of original porosity and grain layout, which is clearly different from the part of the rock not affected with the band. The limit of the zone, which is

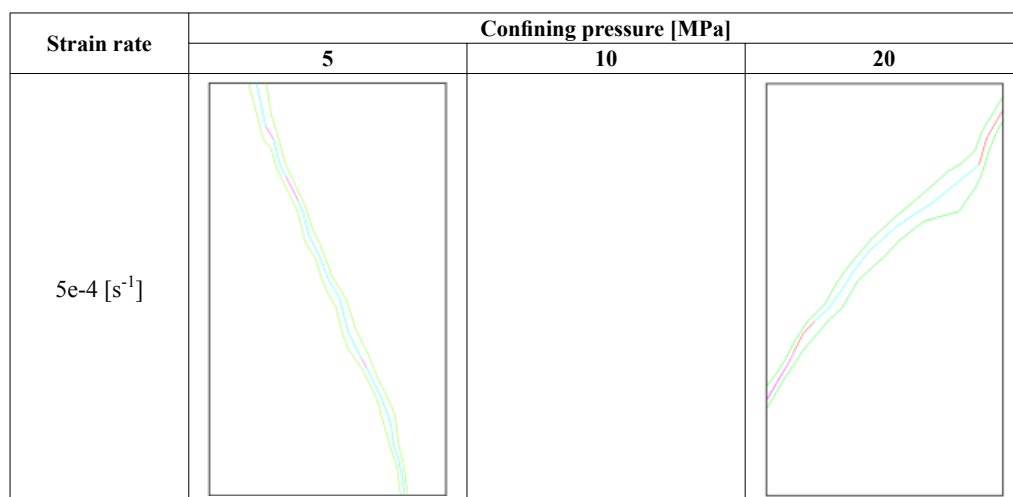
also an effect of the emerging slip band, has been marked in green in Fig. 12. Macroscopically observed shear band where sample damage occurs, in the micro-scale comprises both the shear surface in the form of cataclasis, compaction/loosening, or single fracture, as well as the area, marked in green, of affected original porosity of the sample.

6. Analysis of the form of damage, shape and layout of slip bands on sample facings

Previously characterised phenomena observed under the microscope on sections, corresponding to different strain conditions, have been presented in drawings and collected in Table 2.

TABLE 2

Strain rate	Confining pressure [MPa]		
	5	10	20
1e-5 [s ⁻¹]			
1e-4 [s ⁻¹]			



It must be pointed out that shear bands illustrated in sections map the shear surface just in one cross-section and are not images of the entire band. Drawings presented indicate that within one facing, locally, shear bands feature varied thickness and orientation. What is more important, within one band, in its various sections, several phenomena can be observed: cataclasis, compaction, as well as single fracture. In the case of several shear bands in one sample, their slanting against the loading direction is similar, while in the areas of band merger, their thickness significantly increases. Locally, in the case of changes to the slanting of shear band, its thickness increases. Generally, one can state that band slanting depends on confined pressure, and is the greater, the greater the confined pressure. This observation conforms to macroscopic observations and known dependency between the shear angle and confined pressure.

7. Quantitative analysis of phenomena occurring in shear bands

The previously characterised phenomena were analysed quantitatively by two parameters describing: relative length of sections where they are present in each section and relative surface of slip band.

Relative length of segments where particular phenomena occur was calculated by adding lengths of phenomenon occurrence (marked in relevant colour on sections) and by dividing it by the total length of segments of all phenomena present in a particular section (particular sample):

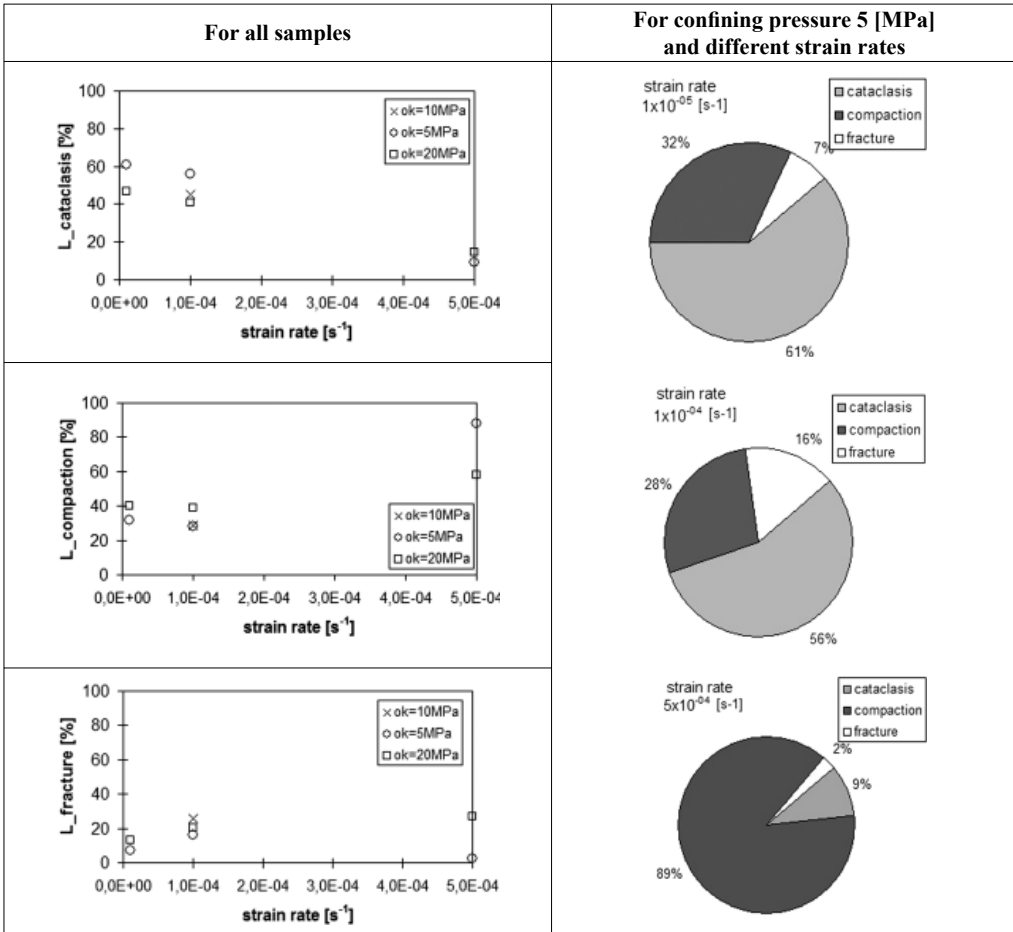
$$L_{cataclasis} = \frac{\sum l_i - cataclasis}{\sum l_i} \cdot 100\%$$

In this manner, percentage share of the effect of the phenomenon analysed (e.g. cataclasis) was obtained in the entire cross-section of the section.

Comparison of the share of particular phenomena in the sample destruction process for various strain conditions has been presented in Table 3.

TABLE 3

Quantitative share of the phenomena of cataclasis, compaction and fractures in limestone samples



The share of particular types of phenomena clearly depends on the strain rate and the confined pressure used in the test. In the right column of Table 3, for confined pressure of $p = 5$ MPa, one can clearly see that the share of cataclasis in the shear band decreases with the growing sample strain rate. It is contrary in the case of the share of compaction, which increases with increased strain rate. The nature of these phenomena is similar both at confined pressure of $p = 5$ MPa, and $p = 20$ MPa (Table 3, left column). For low deformation rates, the share of cataclasis can be determined at the level of 50-60%, while at deformation rates of 5×10^{-4} [s⁻¹], it drops down to approx. 13%. This phenomenon is reverse in the case of compaction. For low strain rates, its share is observed at the level of 30-40%, and grows to 60-90% in the case of strain rates of 5×10^{-4} [s⁻¹]. Percentage share of fractures in the shear band remains at the similar, fixed level, and does not exceed 25% of damage analysed in the section.

Local width of the shear band zone was set as section linking the edges of the band zone, perpendicular to the section marking the direction of cataclasis, compaction or fracture (Fig. 13 to

the left). Fig. 13, to the right, presents histograms of zone widths for particular types of damage in the band.

The analysis of histograms can bring to conclusions that for the sample analysed, the width of shear bands occurring due to compaction in 88%, while for cataclasis in 76% cases, remains within the range of 0.6 – 1 mm. Band width around the fracture in 70% cases does not exceed 8 mm. Locally, in the areas of band mergers, or due to the change of damage nature, the width of the band increases, which results in skew of distributions for all forms of damage.

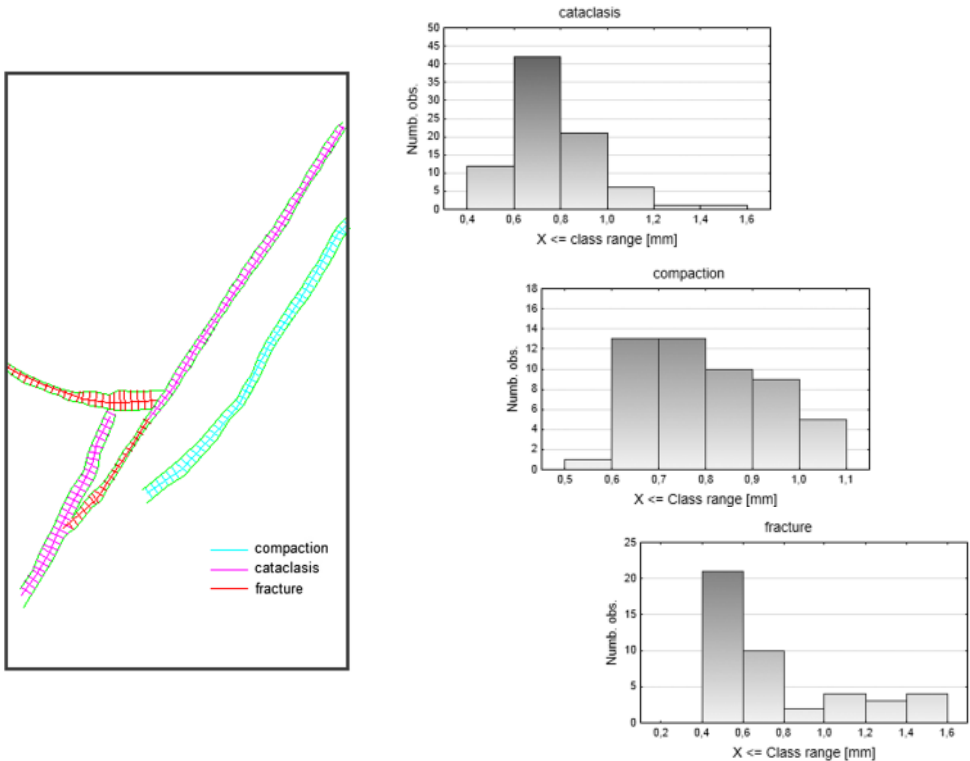


Fig. 13. Widths of shear band zones and their distribution broken to phenomena obtained for exemplary sample ($p = 10$ MPa, deformation rate 1×10^{-4} [s $^{-1}$])

Due to different length of shear bands on various sections (samples), the parameter of shear band surface was also standardised. Relative shear band surface was calculated as the total of products of locally measured zone width and length of the segment where the width occurs, divided by the total length of segments referring to the same type of damage. The parameter obtained thus characterises, to a certain extent, the width of shear band for a particular form of damage, standardised by its length.

$$h_{relative} = \frac{\sum h_i \cdot l_i}{\sum l_i}$$

The main objective of the analyses performed herein was to answer the question of how the width of shear bands changes together with the change of strain rate and at various confining pressures of mechanical tests. The analyses were performed for three analysed confining pressures, whereas in the case of pressure $p = 5$ MPa and 20 MPa, data originate from three samples for each of the pressures, while in the case of $p = 10$ MPa – from one sample.

Shear band surface for all three damage types clearly depends on both strain rate and confining pressure (Fig. 14). The largest band surface was obtained for compaction phenomenon, while slightly smaller for cataclasis. In the latter case, one can also observe its smaller dependency on confined pressure. Generally, one can state that the higher the strain rate, the greater the surface of cataclasis and compaction bands. In the case of compaction, one can also clearly see its dependency on confining pressure, as for higher pressures, the widths of compaction zone are greater than for confining pressure of 5 MPa.

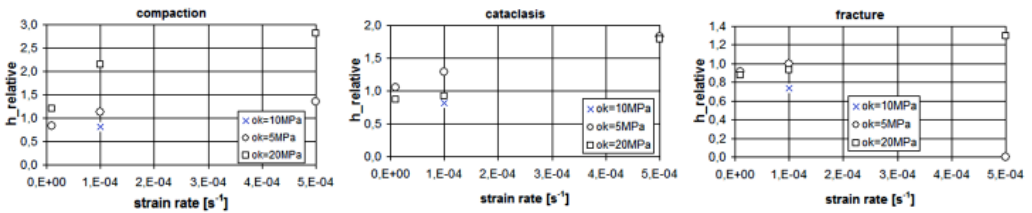


Fig. 14. Relative shear band surface obtained for various strain rates and confined pressures

For various reasons, e.g. in analysis of energy dissipation during sample damage and its association with the widths of zones of permanent deformation location, average width of bands calculated for samples without breaking it into particular types of damage might prove interesting. The results of such analyses have been presented in Fig. 15.

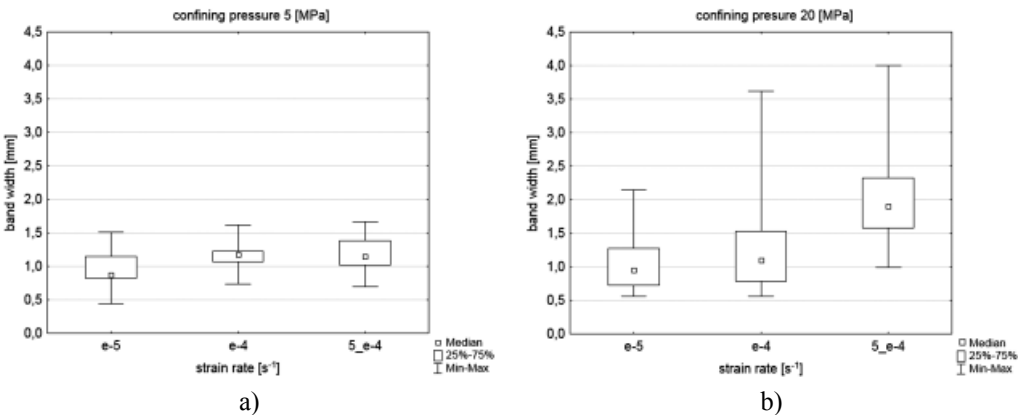


Fig. 15. Actual width of shear bands in the function of confined pressure and deformation rate

For confining pressure of 5 MPa and low strain rates (1×10^{-5} [s⁻¹]), half of measured shear band widths remains within the range of 0.8-1.2 mm, while for deformation rate of 5×10^{-4} [s⁻¹] – within the range of 1-1.4 mm. The differences are not great, but they are statistically significant*. For higher confined pressure of 20 MPa, where distribution skew was rather high, one can observe much greater span of results. In the case of low strain rates (1×10^{-5} [s⁻¹]), the range of band widths was similar to the one obtained for confined pressure of 5 MPa. However, in the case of higher deformation rate (5×10^{-4} [s⁻¹]), half of measured shear band widths practically remained within the range of 1.5-2.3 mm. Differences between the groups are clear and statistically significant*. Attention, however, must be drawn to the fact that locally, in the areas of shear band merger, zone widths were much different from such values, reaching up to 4 mm. The results of this analysis point to clear dependency of shear band width on both strain rate and confining pressure (Fig. 15 a, b).

8. Conclusions

Microscopic analysis of shear bands performed in this article, as present in the Luna limestone samples subjected to quasi-static triaxial loading conditions, has allowed for the assessment of the nature and range of such bands. On the basis of the analyses performed, one can state that within one shear band, there can be various forms of damage, in the form of cataclasis, compaction, and single fracture. Moreover, not far from the phenomena listed, one can also observe the change of original porosity and structure, which is clearly different from the part of the rock not affected with the band. Both the type of damage present in the band, and the width of the shear band itself, depends on loading conditions and, to a smaller extent, also on petrographic properties of the rock analysed. On the basis of the results presented, one can state that the most important factors affecting both the nature of the phenomena observed and their range were strain rate and confining pressure in which the tests were performed. The results of the presented tests on limestone will be used for formulation of the failure surface (plasticity surface), limited in compressive loading space by the “cap” (Rudnicki 2004, Issen & Rudnicki 2000), which in the case of porous rocks allows describing loading conditions for localization in the form of w shear band and compaction band (Bessuelle 2001, Baud et al. 2000). The results obtained for various rates of axial deformation also allow for defining such a condition sensitive to strain rate.

This work have been supported partially by statutory research funds of the AGH University of Science and Technology, Faculty of Mining and Geoengineering within the framework of the research program N^o 11.11.100.197

References

- Amitrano D., Schmittbuhl J., 2002. *Fracture roughness and gouge distribution of a granite shear band*. J. Geophys. Res., Vol. 107, No. B12.
- Baud P., Schubnel A., Wong T.-F., 2000. *Dilatancy, compaction and failure mode in Solnhofen limestone*. J. Geophys. Res., Vol. 195, pp. 19289-19303.

* According to ANOVA Kruskal-Wallis test and mediana test in STATISTICA statistical package. Cardinality for groups compared for 5 MPa (1×10^{-5} [s⁻¹] – 103, 1×10^{-4} [s⁻¹] – 90, 5×10^{-4} [s⁻¹] – 98 cases), for 20 MPa (1×10^{-5} [s⁻¹] – 119, 1×10^{-4} [s⁻¹] – 95, 5×10^{-4} [s⁻¹] – 77 cases)

- Bésuelle P., 2001. *Evolution of Strain Localisation with Stress in a Sandstone: Brittle and Semi-Brittle Regimes.*, Phys. Chem. Earth (A), Vol. 26, No. 1-2, pp. 101-106.
- Bésuelle P., Baud P., Wong T.-F., 2003. *Failure Mode and Spatial Distribution of Damage in Rothbach Sandstone in the Brittle-ductile Transition*, Pure Appl. Geophys., 160, 851-868.
- Bésuelle P., Desrues J., Raynaud S., 2000. *Experimental characterization of the localization phenomenon inside a Vosges sandstone in a triaxial cell*. Int. J. Rock Mech. & Mining Sci., Vol. 37, pp. 1223-37.
- Desrues J., 2004. *Tracking Strain Localization in Geomaterials Using Computerized Tomography*, in: X-ray CT for Geomaterials, Otani, J. and Obara, Yuzo Ed., Balkema, pp. 15-41.
- Desrues J., Viggiani G., 2004. *Strain localization in sand: an overview of the experimental results obtained in Grenoble using stereophotogrammetry*. Int. J. Numer. Anal. Meth. Geomech., Vol. 28, pp. 279-321.
- Dunham R.J., 1962. *Classification of carbonate rocks according to depositional texture*, in: Ham W.E. Classification of carbonate rocks. American Association of Petroleum Geologists Memoir. 1. pp. 108-121.
- El Bied A., Sulem J., Martineau F., 2002. *Microstructure of shear zones in Fontainebleau sandstone*. Int. J. Rock Mech. Min. Sci., Vol. 39, 7, 917-932.
- Folk R.L., 1959. *Practical petrographic classification of limestones*. American Association of Petroleum Geologists Bulletin, Vol. 43, p. 1-38
- Folk R.L., 1968. *Petrology of Sedimentary Rocks*. Austin. University of Texas Publication.
- Gustkiewicz J., Gamond J.F., Carrio-Schaffhauser E., 2007. *Variations of the Mechanical Properties of a Sandstone Due to Deformation and Confining Pressure, in Relation to Microstructures*, Arch. Min. Sci., Vol. 52, No 4, p. 505-534.
- Hallbauer D.K., Wagner K., Cook N.G.W., 1973. *Some observations concerning the microscopic and mechanical behavior of quartzite specimens in stiff, triaxial compression tests*. Int. J. Rock Mech. Min. Sci., Vol. 10, 713-726.
- Issen K.A., Rudnicki J.W., 2000. *Conditions for compaction bands in porous rock*. J. Geophys. Res., Vol. 105, pp. 21529-21536.
- Klein E., Baud P., Reuschle T., Wang T.-F., 2001. *Mechanical Behaviour and Failure Mode of Bentheim Sandstone Under Triaxial Compression*. Phys. Chem. Earth (A), Vol. 26, No. 1-2, pp. 21-25.
- Louis L., Wong T.-F., Baud P., Tembe S., 2006. *Imaging strain localization by X-ray computed tomography: discrete compaction bands in Diemelstadt sandstone*. Journal of Structural Geology 28, 762-775.
- Olsson W., Peng S., 1976. *Microcrack nucleation in marble*. Int. J. Rock Mech. Min. Sci. & Geomech. Abstr., Vol. 13, 53-59.
- Ord A., Vardoulakis I., Kajewski R., 1991. *Shear band formation in Gosford sandstone*. Int. J. Rock Mech. Min. Sci. & Geomech. Abstr., Vol. 28, 5, 397-409.
- Paterson M.S., Wong T.-F., 2005. *Experimental rock deformation - the brittle field*, Second Edition, Springer.
- Renner J., Rummel F., 1996. *The effect of experimental and microstructural parameters on the transition from brittle failure to cataclastic flow of carbonate rocks*. Tectonophysics, 258 151-169.
- Rudnicki J.W., 2004. *Shear and compaction band formation on an elliptic yield cap*. J. Geophys. Res., Vol. 109, Iss. B3.
- Tondi E., Atonellini M., Aydin A., Marchegiani L., Cello G., 2006. *The role of deformation bands, stylolites and sheared stylolites in fault development in carbonate grainstones of Majella Mautain, Italy*. Journal of Structural Geology 28, Issue 3, 376-391.
- Vajdova V., Zhu W., Chen T.-M.N., Wong T.-F., 2010. *Micromechanics of brittle faulting and cataclastic flow in Tavel limestone*. Journal of Structural Geology 32, 1158-1169.
- Viggiani G., Lenoir N., Bésuelle P., D.M., Desrues J., Kretschmer M., 2004. *X-ray micro tomography for studying localized deformation in fine-grained geomaterials under triaxial compression*, Comptes rendus Mécanique, Académie des Sciences vol. 332 , pp. 819-826.
- Wong T.-F., 1982. *Micromechanics of faulting in westerly granite*. Int. J. Rock Mech. Min. Sci. & Geomech. Abstr., Vol. 19, Issue 2, pp. 143-160.
- Wub X.Y., Bauda P., Wong T.-F., 2000. *Micromechanics of compressive failure and spatial evolution of anisotropic damage in Darley Dale sandstone*. Int. J. Rock Mech. Min. Sci., Vol. 37, 143-160.

Received: 17 December 2012